Journal of Applied Physics PERSPECTIVE scitation.org/journal/jap

Multi-junction solar cells paving the way for super high-efficiency

Cite as: J. Appl. Phys. **129**, 240901 (2021); doi: 10.1063/5.0048653
Submitted: 25 February 2021 · Accepted: 1 June 2021 ·
Published Online: 23 June 2021

View Online Export Citation CrossMark

Masafumi Yamaguchi,[1,a)] Frank Dimroth,[2] John F. Geisz,[3] and Nicholas J. Ekins-Daukes[4]

AFFILIATIONS

[1]Toyota Technological Institute, Nagoya 468-8511, Japan
[2]Fraunhofer Institute for Solar Energy Systems ISE, Freiburg 79110, Germany
[3]National Renewable Energy Laboratory, Golden, Colorado 80401, USA
[4]School of Photovoltaic & Renewable Energy Engineering, University of New South Wales, Sydney 2052, Australia

[a)]**Author to whom correspondence should be addressed:** masafumi@toyota-ti.ac.jp

ABSTRACT

In order to realize a clean energy society by using renewable energies, high-performance solar cells are a very attractive proposition. The development of high-performance solar cells offers a promising pathway toward achieving high power per unit cost for many applications. As state-of-the-art of single-junction solar cells are approaching the Shockley–Queisser limit of 32%–33%, an important strategy to raise the efficiency of solar cells further is stacking solar cell materials with different bandgaps to absorb different colors of the solar spectrum. The III–V semiconductor materials provide a relatively convenient system for fabricating multi-junction solar cells providing semiconductor materials that effectively span the solar spectrum as demonstrated by world record efficiencies (39.2% under one-sun and 47.1% under concentration) for six-junction solar cells. This success has inspired attempts to achieve the same with other materials like perovskites for which lower manufacturing costs may be achieved. Recently, Si multi-junction solar cells such as III–V/Si, II–VI/Si, chalcopyrite/Si, and perovskite/Si have become popular and are getting closer to economic competitiveness. Here, we discuss the perspectives of multi-junction solar cells from the viewpoint of efficiency and low-cost potential based on scientific and technological arguments and possible market applications. In addition, this article provides a brief overview of recent developments with respect to III–V multi-junction solar cells, III–V/Si, II–VI/Si, perovskite/Si tandem solar cells, and some new ideas including so-called 3rd generation concepts.

I. INTRODUCTION

The development of high-performance solar cells offers a promising pathway toward achieving high power per unit cost for many applications. Various single-junction solar cells have been developed and efficiencies of 29.1%, 26.7%, 23.4%, 22.1%, and 21.6% (a small area efficiency of 25.2%) have been demonstrated[1] with GaAs, Si, CIGSe, CdTe, and perovskite solar cells, respectively. However, single-junction solar cells may be capable of attaining AM1.5 efficiencies of up to 30%–32%, as shown in Fig. 1.[2] That is, state-of-the-art of single-junction solar cells are approaching the Shockley–Queisser limit.[3] An important strategy to raise the efficiency of solar cells is stacking solar cell materials with different bandgaps to absorb different colors of the solar spectrum. This so-called multi-junction (MJ)[4,5] approach can reduce thermalization loss due to a high-energy photon absorbed by a small-bandgap material and below-bandgap loss due to a low-energy photon of insufficient energy to excite an electron in a high-bandgap material, as shown in Fig. 2.[6] Figure 3 shows the principle of wide photoresponse using MJ solar cells for the case of a triple-junction solar cell.[7] Solar cells with different bandgaps are stacked one on top of the other so that the solar cell facing the sun has the largest bandgap (in this example, this is the GaInP top solar cell with a bandgap energy Eg of 1.8–1.9 eV). This top solar cell absorbs all the photons at and above its bandgap energy and transmits the less energetic photons to the solar cells below. The next solar cell in the stack (here the InGaAs middle solar cell with an Eg of 1.41 eV) absorbs all the transmitted photons with energies equal to or greater than its bandgap energy and transmits the rest downward in the stack (in this example, to the Ge bottom solar cell with an Eg of 0.67 eV). Of all the so-called third generation solar cell strategies,[8] only MJ designs have been successful in surpassing the detailed-balance limit of single-junction solar cells. Such successful

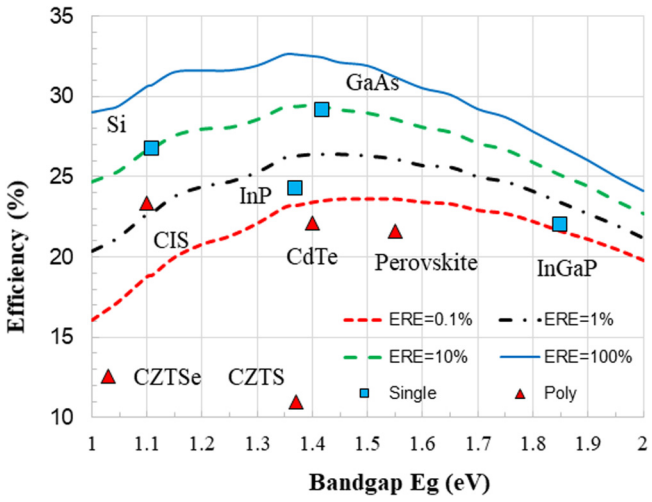

FIG. 1. Calculated and obtained efficiencies of single-junction single-crystalline and polycrystalline solar cells. ERE shows external radiation efficiency expressed by Eq. (1), and the solar cells with the higher ERE value show a reduced non-radiative recombination loss. The efficiency values of cells with an area of 1 cm^2 or larger area are plotted in the figure. Reproduced with permission from Phys. Status Solidi C **12**, 489 (2015). Copyright 2015, Wiley.

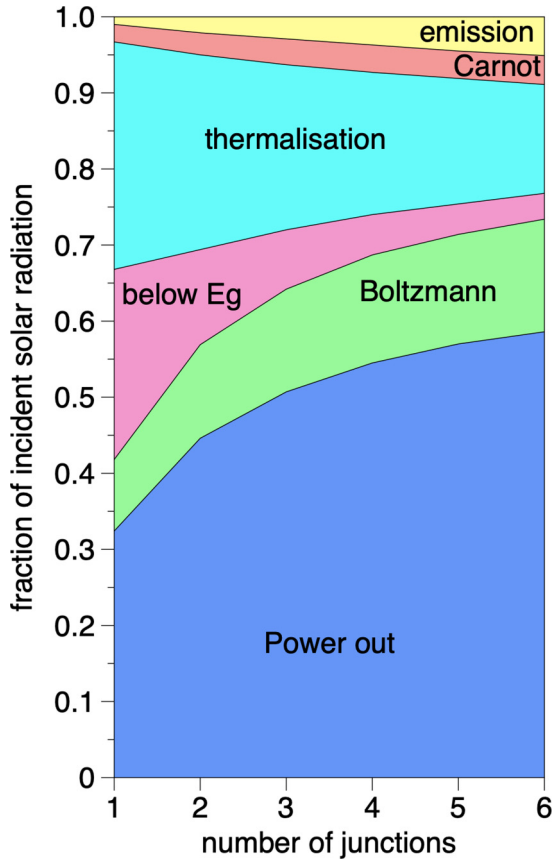

FIG. 2. Loss processes and powerout in an unconstrained MJ device under one-sun illumination (6000 K blackbody) are shown. All incident solar radiation is accounted for. Optimal bandgaps are used in each case. All mechanisms are shown to be dependent on the number of junctions. Adapted with permission from Prog. Photovolt. **19**, 286 (2011). Copyright 2011, Wiley.

achievements are thought to be due to longtime R&D since the late 1970s, bandgap engineering including lattice matching, high-quality epitaxial growth, and so forth.

The operating principles of MJ solar cells were suggested by Jackson[9] as long ago as 1955, and they have been investigated since 1960.[10] This concept was most successfully implemented in III–V compound semiconductor solar cells, since a compound semiconductor has a good range of lattice parameters and bandgaps to choose from. High efficiencies of 32.8%[1] under one-sun and 35.5%[11] under concentration with two-junction solar cells, 37.9%[12] under one-sun and 44.4%[12] under concentration with three-junction solar cells, 46.1%[13] under concentration with four-junction solar cells, 38.8%[14] under one-sun with five-junction solar cells, and 39.2%[15] under one-sun and 47.1%[15] under concentration with six-junction solar cells have been demonstrated, as shown in Fig. 4 and Fig. 6. Figure 4 shows the chronological improvement in conversion efficiency[7,16] of concentrator MJ and one-sun MJ solar cells in comparison with those of crystalline Si, GaAs, CIGS, and perovskite single-junction solar cells.

In the days to come, Si-based tandem solar cells[16] such as III–V/Si,[17,18] II–VI/Si,[19] chalcopyrite/Si,[20] CZTS/Si,[21] and perovskite/Si[22] tandem solar cells are expected to play a more important role as high-efficiency, low-cost solar cells move closer to industrial manufacturing. In addition, there are other approaches such as perovskite/perovskite,[23] III–V/CIGSe,[24] and perovskite/CIGSe[25] MJ solar cells that are still at a lower technology readiness level but may become very attractive candidates for photovoltaic energy conversion in the future.

Here, we discuss the perspectives of MJ solar cells from the viewpoint of efficiency and low-cost potential based on scientific and technological arguments and possible market applications. In addition, this article provides a brief overview of recent developments with respect to III–V MJ solar cells, III–V/Si, II–VI/Si, perovskite/Si tandem solar cells, and some new ideas including so-called 3rd generation concepts.[8]

II. SCIENTIFIC CONSIDERATION

The fundamental processes in photovoltaic power conversion are shown in Fig. 5, where incident sunlight of energy above the semiconductor bandgap can be absorbed (1) and excess energy dissipated as a thermalization loss (3); photons below the bandgap energy can pass through the solar cell unabsorbed (2). Excess radiative recombination proceeds due to the presence of photogenerated carriers (4). At forward operating voltages, the free energy of the carriers is determined by the quasi-Fermi level separation that defines the solar cell voltage at the electrical contacts to the solar cell, $V = \mu e - \mu h$.

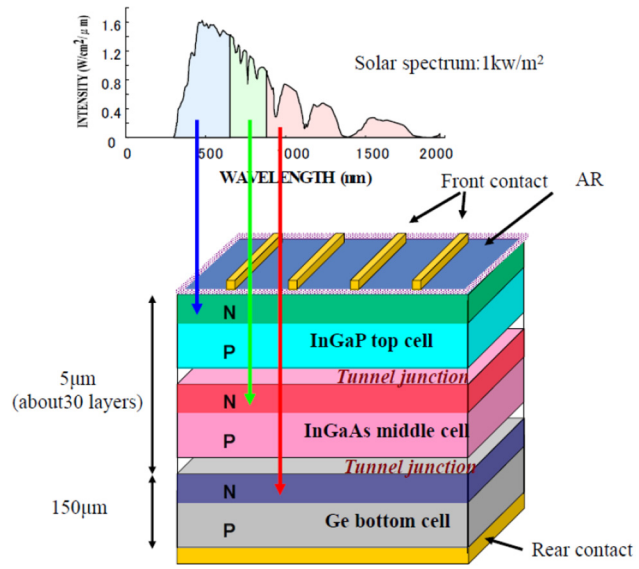

FIG. 3. Principle of wide photoresponse by using a MJ solar cell, for the case of an GaInP/InGaAs/Ge triple-junction solar cell. Adapted with permission from M. Yamaguchi, "High-efficiency GaAs-based solar cells," in *Gallium Arsenide*, edited by T. Tabbakh (IntechOpen, 2020). Copyright 2020 Toyota Technological Institute.

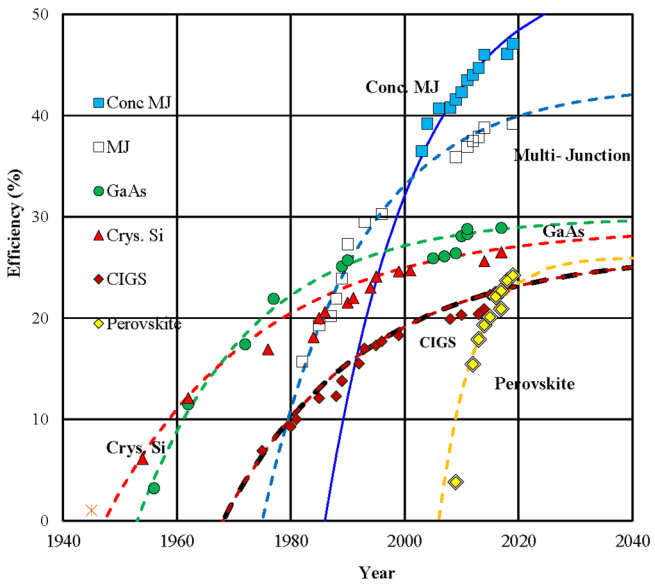

FIG. 4. Chronological improvements in the conversion efficiencies of concentrator MJ and MJ solar cells in comparison with those of crystalline Si, GaAs, CIGS, and perovskite single-junction solar cells. Adapted with permission from M. Yamaguchi, "High-efficiency GaAs-based solar cells," in *Gallium Arsenide*, edited by T. Tabbakh (IntechOpen, 2020). Copyright 2020 Toyota Technological Institute.

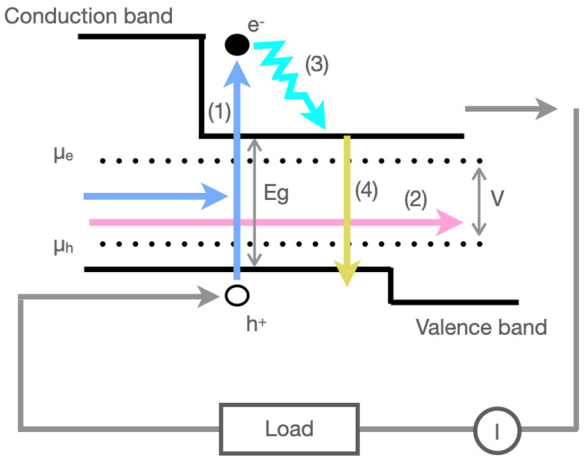

FIG. 5. Fundamental processes in an ideal solar cell: Schematic of a single-junction solar cell of bandgap Eg showing four fundamental processes: (1) absorption of light above the bandgap energy (Eg), (2) transmission of light below the bandgap energy, (3) thermalization of excess energy, and (4) radiative recombination.

The breakdown between power generated by the solar cell and these losses is illustrated in Fig. 2.[6] For a single-junction solar cell, the two largest losses are the thermalization and below-Eg losses, both of which are significantly mitigated with the addition of semiconductor junctions with different bandgap energies in an MJ device. This is because a larger portion of the solar spectrum is then absorbed close to the bandgap of one of the semiconductors and, therefore, experiences less thermalization of carriers. All other fundamental losses (note that resistance losses are not regarded as fundamental losses, though they are unavoidable in practical devices and, in fact, benefit from lower currents that are typically achieved with more junctions) increase with an increased number of semiconductor junctions and are discussed in detail elsewhere.[3] We note that all three remaining losses fundamentally depend on solar cell temperature and can, therefore, be reduced by operating the solar cell at a lower temperature.

The so-called "Boltzmann loss" is an entropic loss associated with the increase in the occupancy of optical modes on re-emission of light that results in a voltage loss. Practically, it can be recovered in two ways, conventionally by increasing the solar concentration on the solar cell, or equivalently, by restricting the radiative emission from the cell. Dividing up the solar spectrum between an increasing number of junctions results in emission at multiple wavelengths and hence a larger Boltzmann loss. The loss can be mitigated by paying attention to the geometrical optical arrangement, for example, through solar concentration or an angular restriction of radiative recombination.

The Carnot loss arises from establishing carriers at finite temperature in a band and, hence, rises as further junctions establish additional bands occupied by photogenerated carriers. The loss cannot be recovered except in very unusual circumstances where the PV cell is operated at low temperatures.

The emission loss is unavoidable in a conventional solar cell owing to the reciprocity[26] between absorption and emission encapsulated by Kirchoff's law of radiation. The detailed-balance limit[3] considers only this unavoidable radiative recombination loss through thermodynamic arguments. The external radiative efficiency (ERE) describes how closely a sub-cell comes to this thermodynamic limit as all other non-radiative recombinations are considered potentially avoidable. In an optimally configured MJ solar cell, the emissive loss is small, but in a series-connected tandem solar cell where current flow is constrained by one sub-cell, there can be a significant transfer of energy down the tandem absorber stack. This is known as radiative coupling and discussed in more detail below. An extreme case of radiative coupling arises if the reciprocity between absorption and emission is lifted, potentially using magneto-optical materials,[27] which allows the efficiency of an infinite tandem stack (asymptotes to 86.8%) to be raised to the Landsberg efficiency of 93.5%. At the Landsberg limit, each of the component junctions operates arbitrarily close to Voc and electrical power delivered from the solar cell infinitesimally slowly.[28]

To achieve efficient operation, the photogeneration rates in a series-connected solar cell should be closely matched. While the choice of the bandgap and, hence, absorption threshold for the component junctions plays a primary role, the sub-cell photogeneration can be optimized by adjusting the thickness of the junctions such that an overperforming sub-cell can allow some light to pass unabsorbed into an underlying junction.[29] This approach works well for static solar spectra (such as AM0), but for the terrestrial spectrum, the spectral irradiance varies throughout the day and between seasons with noticeable effects on system performance.[30] If the semiconductor material is radiatively efficient, sub-cells with excessive photogeneration will radiate the excess into lower lying junctions with a small fraction of this escaping from the top of the solar cell. Radiative dominated behavior has been observed in III–V solar cells[31] and some perovskite materials,[32] even appearing as a measurement artifact in MJ devices.[33,34] Since radiative coupling transfers energy down the MJ stack, the effect can mitigate the effects of spectral mismatch under blue-rich spectral conditions[35] as well as offering some freedom in tolerable absorber bandgap configuration,[36] in particular enabling efficient operation of higher-gap top solar cells in a silicon-based tandem.[37]

III. BRIEF OVERVIEW

A. III–V MJ

III–V semiconductor materials have many advantages for high-efficiency solar cells in general and the MJ solar cell in particular. III–V semiconductors consist of elements from the group III (Al, Ga, and In) and V (N, P, As, and Sb) columns in the periodic table arranged in a zinc- blend (or wurtzite) crystal structure. The highest single-junction efficiency has consistently remained a GaAs solar cell due to its bandgap matching the solar spectrum and its high ERE, as shown in Fig. 1. III–V alloys (hereafter III–Vs) cover a wide-bandgap range from 2.4 eV down to almost 0.0 eV, as shown in Fig. 6, with III–N alloys covering much higher bandgaps[38] (not shown).

Many of the III–Vs can be grown as *single-crystal layers* on single-crystal substrates (e.g., GaAs, InP, Ge, etc.) using liquid phase epitaxy (LPE), molecular beam epitaxy (MBE), organometallic vapor phase epitaxy (OMVPE), and hydride vapor phase epitaxy (HVPE) techniques. Many III–Vs *can be doped* both n-type and p-type over a wide density range and are direct gap for nearly complete thin-film absorption. They can have *high mobilities*, relatively *long lifetimes*, and *low interface recombination* when higher bandgap alloys are used for heterojunction passivation (i.e., window and back-surface field layers) that result in *diffusion lengths* longer[39] than the required single-pass absorption thicknesses. Thus, light-trapping techniques often used in silicon photovoltaics have not been much required for III–V materials. The primary disadvantage of III–V solar cells is their *sensitivity to defects* that act as deep non-radiative recombination sites, such as dislocations, impurities, and phase boundaries, but they also have a relatively low density if there are intrinsic native defects. While III–Vs can be grown with a high degree of crystal perfection that avoids the problems of defects, it can presently be done only at a relatively high *cost* that results in the other primary disadvantage of III–V solar cells. Due to the high cost of III–V solar cell fabrication, they have been used in applications that leverage the efficiency advantage on the balance of system costs, such as space, concentrator, and other area or weight constrained applications. Concentrator applications have also been intimately tied to III–V MJ development because of the logarithmic increase in voltage with concentration for each junction.

From the beginning of MJ solar cell research, III–V alloys have been the material of choice due to the advantages listed above. In addition, the wide range of bandgaps appropriate for solar collection at the same lattice constant, as shown in Fig. 6, has provided

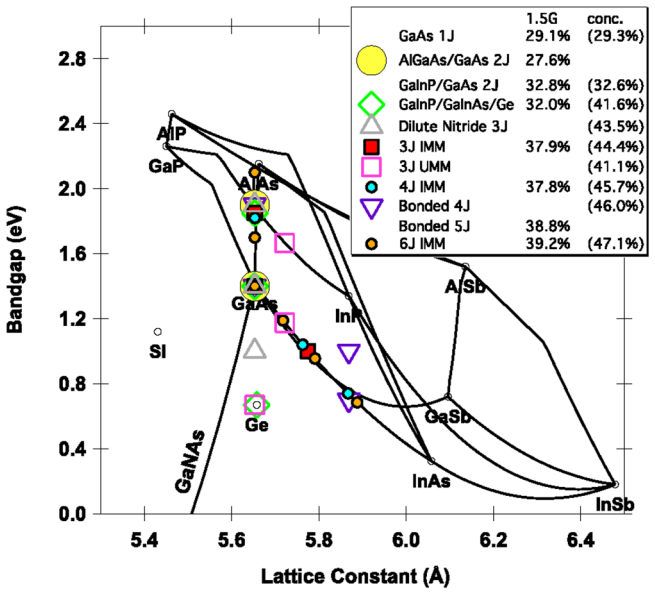

FIG. 6. Bandgap vs lattice constant of III–V semiconductor alloys. Various MJ solar cell combinations are also shown with demonstrated AM1.5 global one-sun and AM1.5 direct concentrator efficiencies. Most successful III–V MJ solar cell designs use GaAs and GaInP junctions.

many avenues for creating defect-free monolithic MJ configurations. Several of the III–V MJ strategies with their achieved efficiencies are summarized in Fig. 6 and mentioned briefly in the following paragraph.

Initially, multi-terminal structures were considered,[40,41] but since low-resistance tunnel junction interconnects consisting of heavily doped wide-bandgap materials have been demonstrated in III–V materials,[42,43] series-connected MJ solar cells have dominated. Such two-terminal devices facilitate the integration of the solar cells into modules and the connection to inverters. Target bandgap combinations for series-connected MJ solar cells have been calculated for specific spectra assuming detailed-balance[44,45] and more realistic ERE limitations.[46] Recently, wafer bonding,[13] transparent conductive oxide layer insertion,[47] and mechanical stacking[17] for MJ solar cell formation have been demonstrated. The first III–V MJ strategy considered was the easily lattice-matched AlGaAs/GaAs structure,[48–50] but difficulties with defects associated with oxygen incorporation into AlGaAs restricted progress.[51] The surprising stability[52] and quality of epitaxially grown GaInP lattice-matched to GaAs finally resulted in the GaInP/GaAs solar cell with an efficiency of 29.5%[53] to exceed the theoretical potential of any single-junction solar cell. Spontaneous ordering in GaInP material also resulted in adjustable bandgaps for the same alloy composition.[54] The use of Ge substrates was primarily introduced to GaInP/GaAs solar cells for the mechanical and cost advantages over GaAs substrates, but the serendipitous introduction of a diffuse Ge junction also resulted in a slight voltage increase without much added cost or complexity. These GaInP/GaAs/Ge three-junction (3J) solar cells have remained the standard for space and concentrator applications to this day. Improvements on this 3J solar cell revolved around replacing the low-Eg Ge junction with a higher-Eg III–V junction. Dilute nitride GaInNAs(Sb) that is lattice-matched to GaAs was a very promising 1.0 eV candidate[55] but sufficient quality was not obtained over many years with industry standard OMVPE growth. Using (arguably) more expensive MBE growth, excellent concentrator 3J solar cells with a dilute nitride bottom junction[56] have been demonstrated.[57] While high densities of threading dislocations (TDD) are detrimental to III–V quality,[58] metamorphic growth (which allows the mismatched strain to be relaxed slowly in compositionally step graded buffer layers) has allowed high-quality lattice-mismatched InGaAs junctions to be grown with TDD$\sim 1\times10^{6}$ cm^{-2} on GaAs substrates. The inverted metamorphic multi-junction (IMM) strategy[59] that grows the low-bandgap InGaAs junctions last has been demonstrated with three,[60,61] four,[62,63] and six junction[15] III–V solar cells with extremely high efficiencies. A natural consequence of the IMM strategy is the removal of the substrate, which has advantages for cost with potential substrate reuse, light-weight, and flexible solar cells,[64,65] and back-surface reflectors for photon recycling.[31,66] The dislocations in mismatched InGaAs could alternatively be isolated from the high-quality top junctions by bifacial growth[67] or through the use of strain-balanced GaAsP/InGaAs bi-layers.[68] The upright, metamorphic growth of lattice-mismatched top junctions on an active Ge junction (UMM) has also been demonstrated with high efficiency.[69,70] Interestingly, very different 3J bandgap combinations used in the 3J IMM[60] and 3J UMM[69] resulted in very similar efficiencies as a result of the absorption gaps in the terrestrial spectra.[46] More recently also, five-junction UMM solar cells were developed and used in concentrator photovoltaics.[71] Even higher quality low-bandgap junctions have been obtained by separately growing lattice-matched junctions on InP and wafer bonding with junctions grown on GaAs substrates for a 4J concentrator [13] and 5J one-sun solar cell.[14] Space solar cells with AM0 efficiencies >32% are available as 4J UMM and 5J IMM structures.

$Ga_{1-x}In_xN$ alloys (that have been successful for light emitting devices using low-In content) have also been suggested for MJ solar cell materials because the alloy theoretically covers the full bandgap range.[38] Some high-bandgap GaInN solar cells have been demonstrated,[72] but the fabrication of the high-In GaInN alloys to capture the infrared portion of the solar spectrum has remained challenging. High-In GaInN alloys suffer from polarization charge,[73] contact inversion layers,[74] phase decomposition,[75] and large lattice mismatch.[76]

B. III–V Si tandem

Silicon is a material that combines multiple benefits. It is earth abundant, almost 30% of the Earth's crust is formed from silicon. It can be purified to extremely high levels (typically less than 0.001% impurities in solar cell material) and grown into mono- or multi-crystalline ingots, which are then diced and processed to solar cell devices absorbing sunlight between 300 and 1200 nm. The bandgap is close to ideal for a single-junction solar cell and has resulted in hero devices with up to 26.7% conversion efficiency.[77] Mechanical strength and stability are further advantages and the cost of silicon solar cells has come down 82% (solar costs have fallen 82% since 2010, https://www.pv-magazine.com/2020/06/03/solar-costs-have-fallen−82-since-2010/) just between 2010 and 2020 mainly due to increased mass manufacturing and economies of scale. Fully processed devices are sold at approximately 0.12 US$/W (prices according to http://pvinsights.com/(27.4.2021)) or 27 US$/m^2 at an average solar-electric conversion efficiency of 22.5% AM1.5g. This is less than the price for many building materials like floor tiles. One could argue that the perfect solar cell material has been already found, but some limitations may still need to be overcome. Being an indirect semiconductor, silicon requires a certain thickness (typically 150 μm) to absorb sunlight, its manufacturing processes are energy intensive, and the conversion efficiency of silicon single-junction solar cells is fundamentally limited to 29.5% by Auger recombination.[78,79] Auger recombination describes the three carrier energy transfer from a photogenerated carrier to an electron in the conduction band and, therefore, becomes even more important at high concentrations. This fundamental intrinsic recombination process determines the charge carrier lifetimes of ultra-pure silicon, different from direct semiconductors like GaAs or GaInP, which are limited by radiative recombination.

The fundamental efficiency limit of silicon single-junction solar cells can be overcome by MJ devices as described above and such solar cells may still benefit from using silicon as the bottom junction and substrate material. This is attractive because most thin-film absorbers need a support as they are too thin to be self-sustained. Also, silicon with a 1.1 eV bandgap is close to the optimum for dual-junction and triple-junction devices. The ideal bandgap energy[80] for one additional absorber above Si is 1.7 and

2.0/1.5 eV in the case of two absorbers. The exact bandgaps depend on several factors such as transparency of the upper layers and the long-wavelength response of the silicon bottom solar cell. In fact, this has turned out to be one of the challenges in manufacturing tandem solar cells on silicon. The light-trapping features have to move from the front to the rear of the wafer to allow the deposition of planar thin-film absorbers at the front.[81–83] This can be done by implementing a pyramid texture,[84] spheres,[85] or nanostructure gratings[86] on the back of the silicon wafer to increase the light path through the silicon and, therefore, enhancing absorption close to the indirect bandgap.

The most successful examples for Si-based tandem solar cells in terms of conversion efficiency are combinations of III–V compounds with Si (see example in Fig. 7 right). GaAsP/Si tandem solar cells have reached AM1.5g conversion efficiencies of 23.4% (monolithic, two-terminals),[87,88] GaAs/Si up to 32.8% (four-terminal),[17] and GaInP/Ga(In)As(P)/Si up to 35.9% (two-terminal[89,90] and four-terminal).[17] Some groups are involved in growing the III–V layers directly on silicon, which is a challenge due to the large difference in the lattice constant of 3%–4% and thermal expansion coefficient. Other groups have used wafer bonding or gluing to make the connection, followed by a removal of the growth substrate. Of course, the latter can be economically attractive only if the growth substrate is removed with high yield and reused for the further growth of III–V layers.[91] Direct growth of the III–V absorbers onto silicon using methods like metal-organic vapor phase epitaxy is challenging in terms of achieving low enough defect densities for highest efficiency devices, but continuous progress is being made in the field of metamorphic III–V growth on silicon.[92,93] With further research, this problem may be solved in the near future, making III–V direct growth the method of choice for realizing tandem solar cells on silicon that combine high performance and reliability and that can be manufactured at competitive costs.

C. Other MJ architectures

The ideal attribute for a MJ sub-cell material is one whose absorption threshold can be tuned over the solar spectrum, is stable, non-toxic, and efficient, and can be integrated into a tandem stack at low cost. The integration of sub-cells poses a particularly awkward challenge, since sub-cells that can perform well in isolation can become impaired when integrated with additional sub-cells, either via impurity diffusion or via an excessive thermal budget. Mechanically stacking separate sub-cells in a multi-terminal device is one means by which incompatibilities can be overcome and serves as a useful proof of concept. For brevity, we survey here only two-terminal tandem solar cells fabricated from at least one novel material.

Metal halide perovskite materials are strong, direct-gap semiconductors with optical absorption, typically extinguishing sunlight in a layer of 200–400 nm thickness. Their absorption threshold can be tuned over a wide wavelength range owing to the wide range of alloy combinations with a ABX3 structure, where A is an organic amine cation, B is the metal cation, and X is the halide anion. Typical choices for A are methylammonium iodide or formamidinium iodide Cs, B is commonly Pb and/or Sn, and X is a halide, typically I and/or Br, resulting in compounds such as $(FA_{0.75}Cs_{0.25})Pb(I_{0.8}Br_{0.2})_3$ a popular material for the top solar cell of a tandem. These materials offer a tantalizing and unprecedented range of photovoltaic solar cell absorber material combinations that can be prepared both via solution processing or via vapor deposition.[94] Several permutations of perovskite tandem have been attempted[95] and, in particular, the material system offers a range of opportunities for achieving wide-gap absorbers that are well suited for many tandem solar cell applications.[96]

1. Perovskite/silicon tandems

The versatility of the perovskite material has made it a popular choice for a silicon tandem architecture as a top solar cell with a potentially facile preparation, as illustrated in Fig. 7 (left). In this popular and fast-moving field, the aim is to establish a stable, wide-gap perovskite material[96,97] that is compatible with a suitable silicon bottom solar cell.[98] One of the outstanding challenges is to improve the voltage of the wide-gap perovskite top cell.[95]

A 29.2% perovskite/silicon tandem solar cell was achieved by spin-coating a 1.68 eV perovskite material onto a n-type heterojunction silicon solar cell with a textured rear only. Interconnection

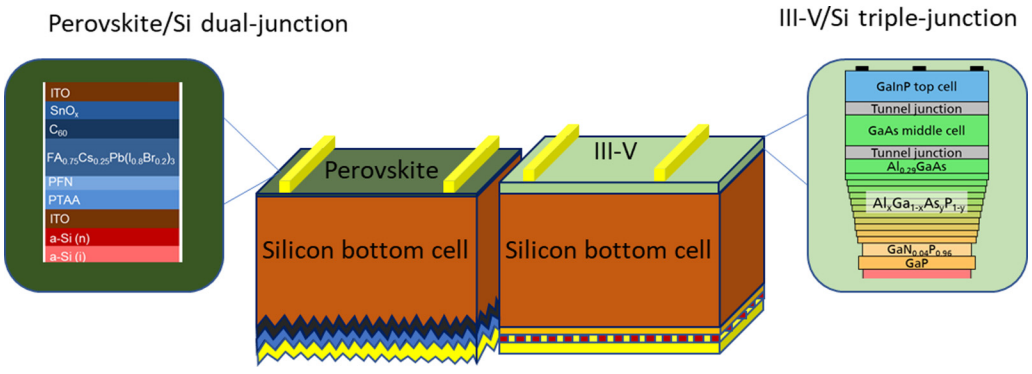

FIG. 7. Examples for the layer structure of a perovskite/Si dual-junction solar cell structure with pyramids on the rear (left) and a GaInP/GaAs/Si triple-junction solar cell that uses a nanostructured resist grating as a diffusor on the back (right).

between the silicon and perovskite material was achieved using a transparent, conducting metal-oxide ITO layer rather than a tunnel junction.[47] The device was stable under testing, retaining 95% of its initial efficiency after 300 h of operation. An announcement of a 29.5% tandem solar cell was also recently made, but no technical details are available at the time of writing (https://www.pv-tech.org/news/oxford-pv-pushes-tandem-shj-perovskite-cell-conversion-efficiency-to-record-29.52). A double textured perovskite/ n-type heterojunction silicon tandem solar cell achieved a 25.2% power conversion efficiency where perovskite precursors were co-evaporated to form a conformal film over the textured silicon surface and interconnected using a nanocrystalline silicon tunnel junction.[99] A similar result, 25.7%, has also been achieved using a solution processed perovskite absorber and metal-oxide interconnection layer.[100]

2. Perovskite/CIGS tandems

Copper Indium Gallium Selenide (CIGS) solar cells can also provide a convenient and commercially mature low-gap solar cell with strong absorption that, with certain alloy fractions, delivers lower energy band-edge than silicon. The thin absorber enables thin, flexible solar cells to be made[101] and wide-gap perovskite materials offer an opportunity to augment the efficiency in a tandem configuration. Generally speaking, the film roughness of CIGS has complicated the fabrication of efficient tandem devices. The first reported perovskite/CIGS tandem solar cell used a thick PEDOT:PSS layer, achieving an efficiency of 10.9%,[102] and later, the CIGS was polished to yield a smooth surface and a much higher efficiency of 22.4%.[103] More recently, self-assembled monolayers have been shown to form an effective interfacial layer between the perovskite and the rough CIGS material, resulting in a tandem efficiency of 24.2%.[104,105]

3. Perovskite/perovskite tandems

Absorption thresholds as low as 1.2 eV can be achieved using mixed Pb–Sn perovskite materials[106] offering the opportunity for a perovskite/perovskite tandem solar cell. A 24.8% 1.77/1.22 eV perovskite tandem solar cell has been achieved by paying particular attention to Sn oxidation and a low-optical loss tunnel junction that employed an ALD deposited SnO2 layer interlayer between solar cells.[107]

4. Organic tandems

The principal challenge for fabricating organic solar cells has been to find molecular absorber materials that operate efficiently in the infrared wavelength range.[108] A 1.72 eV PBDB-T:F-M/1.26 eV PTB7-Th:O6T-4F:PCBM device achieved an efficiency of 17.3%.[109] In comparison with the perovskite/perovskite tandem solar cell above, the principal loss in this organic tandem device is the low solar cell voltages obtained for each sub-cell, in addition to a marginally impaired External Quantum Efficiency (EQE) and solar cell fill factor.

5. Chalcopyrite tandems

Fully inorganic thin-film tandems can be made using chalcopyrite materials, and the well-established CIGS solar cell material is one alloy combination from a large array of the penternary $(In_{1-x}Ga_x)(S_ySe_{1-y})_2$ material system that can span 1–2.43 eV.[110] A mechanical stack composed of a 1.48 eV CdTe/0.95 eV $CuInS_2$ double junction achieved an efficiency of 15.3%.[111] A 1.68 eV $CuGaSe_2$/1.1eV $CuInGaSe_2$ mechanically stacked device achieved an efficiency of 8.5%[112] while a 1.89 eV GaInP/1.42 eV GaAs/1.20 eV CIGSe mechanically stacked tandem has achieved 24.2%.[113] Combining CIGS films into a monolithic tandem structure has proven difficult, owing to the complexity of forming the second junction without impairing the performance of the first. Alloying with Ag has provided a new dimension to tackle this problem, since Ag alloys not only have marginally higher bandgaps, their lower melting point temperature also helps reduce the thermal budget for forming the tandem solar cell and reduces compositional disorder.[114] Monolithic tandem efficiencies remain low (~3%)[115] but the potential to exceed 25% with this approach exists if the difficulties associated with sub-cell integration can be overcome.[116] Monolithic chalcopyrite tandem devices on silicon have been attempted, and a 1.65 eV Cu_2ZnSnS_4 (CZTS)/ 1.1 eV Si tandem achieved an efficiency of only 3.5%, likely limited by incomplete sulfurization and inadvertent silicon solar cell degradation.[21]

Higher efficiencies have been obtained for a 1.8 eV CdZnTe/ 1.1 eV Si tandem device, which achieved an efficiency of 17%.[19]

6. Antimony chalcogenide tandems

Antimony selenosulfide $Sb_2(S,Se)_3$ forms 1D ribbons[117] and by varying the Se/S atomic ratio, offers an adjustable absorption threshold from 1.7 to 1.1 eV. To date, a 10% efficient single-junction solar cell has been demonstrated[118] and a proof-of-concept 1.74 eV Sb_2S/1.22 eV SbSe achieved an efficiency of 7.9%.[119]

7. Organic-silicon tandems

Organic absorber materials are well suited for absorbing visible wavelengths and can, therefore, form the high bandgap junction in a hybrid organic-silicon device. A dye sensitized solar cell was partnered with a silicon solar cell to form a 1.8 eV dye/1.1 eV Si mechanical stack tandem cell with an efficiency of 14.7%.[120] The convention for the interconnection of a tandem solar cell is a series connected stack, but this is only one means by which multiple absorbers can be arranged, and several other permutations are possible in a combination of series and/or parallel connection.[121] Specifically, the combination of a wide-gap solar cell in parallel with two lower gap solar cells has the merit of lower sensitivity to variation in the incident solar spectrum[122] and this has been demonstrated as a so-called "voltage matched" tandem whereby a pentacene layer absorbs photons at energies above 1.8 eV that undergo singlet fission to produce two electron hole pairs.[123] A fully parallel singlet fission device has also been demonstrated[124] in addition to a conventional series-connected tandem.[125]

All the results reported in Sec. III.C are derived from small area cells, cells that are much smaller than 1 cm^2. For all these approaches to achieve their practical potential, high efficiency will need to be maintained over large areas. III–V multi-junction solar cells are manufactured on 6-in. wafers and subsequently interconnected in series to form a module. The promise of thin-film

tandem cells to which all but the silicon-based tandems aspire, is to expand the substrate size significantly, ideally coating an entire sheet of module glass. One of the few tandem technologies that achieved this on a manufacturable scale was the micromorph tandem from Oerlikon, where an amorphous silicon a-Si/micro-crystalline silicon μc-Si tandem configuration was manufactured over an area of 1.4 m^2 delivering an i initial 11% module efficiency. The micromorph technology was rendered obsolete when the costs of the more efficient c-Si modules dropped significantly below that of the micromorph tandem.

IV. PERSPECTIVE

A. Efficiency improvement and cost reduction potential of MJ solar cells

1. High-efficiency potential of MJ solar cells

An analysis of the performance of MJ solar cells has been carried out by several researchers.[126–134] Figure 8 shows the calculated efficiency potential of MJ solar cells under one-sun and concentration conditions as a function of the number of junctions reported by some groups.[133,134] As shown in Fig. 8, increasing the number of junctions, that is, increasing the number of sub-cells in MJ solar cells is effective for increasing the conversion efficiency of these solar cells. Single-junction and three-junction solar cells have potential efficiencies of more than 50% and 60% under one-sun illumination in the ideal detail-balance limit, respectively. However, only 80% and 85% of ideal efficiencies are pointed out to be achievable in practical devices.[133] Figure 9 shows the calculated efficiencies of III– V compound MJ solar cells under one-sun conditions as a function of the number of junctions and external radiative efficiency (ERE) in comparison with efficiency data (best laboratory efficiencies) reported in Refs. 11–15 and 135 Ideal efficiencies of MJ solar cells can be calculated by estimating the short-circuit current density of sub-cells from the standard solar spectrum, by considering only radiative recombination loss

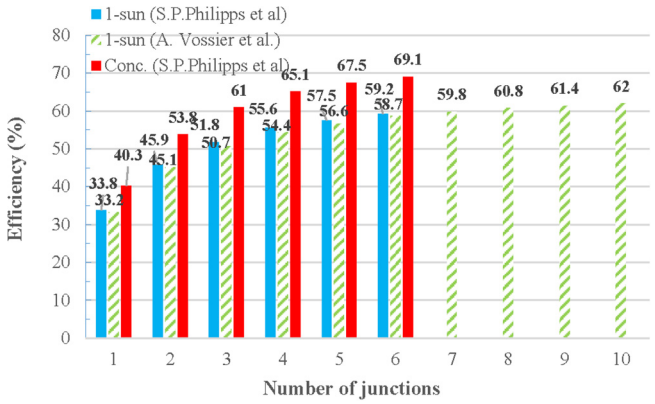

FIG. 8. Calculated efficiencies of MJ solar cells under one-sun and concentration conditions as a function of the number of junctions. Calculated efficiency values are taken from Refs. 132 and 133.

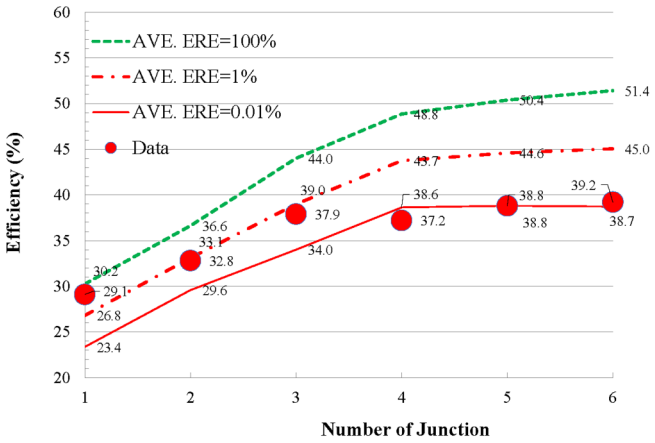

FIG. 9. Calculated efficiencies of III–V compound MJ solar cells under one-sun conditions as a function of the number of junctions and external radiative efficiency (ERE) in comparison with efficiency data (best laboratory efficiencies) reported in references.

(0.26 V loss for Si and 0.28 V loss for GaAs compared with E_g/q: Eg are the bandgap energies of sub-cells, and q is the electronic charge)[136] in sub-cells and resistance loss (only 1%) and similar potential efficiencies of MJ solar cells with reported values[133,134] can be estimated. In the more realistic case, the combination of sub-cells is often selected by considering lattice matching of sub-cell lattice constants and ease of sub-cell material growth. Mismatching of short-circuit current densities of sub-cells by considering bandgap energy and layer thickness of sub-cells, non-radiative recombination, and resistance losses are further considered. In the case of MJ tandem solar cells, we define average ERE (ERE_{ave}) by using average open-circuit voltage Voc loss,

$$\Sigma(V_{oc,n} - V_{oc,rad,n})/n = (kT/q)\ln(ERE_{ave}), \quad (1)$$

where Voc is the measured open-circuit voltage, $V_{occ,rad}$ is the radiative open-circuit voltage, n is the number of junctions, k is the Boltzmann constant, and T is the absolute temperature. The resistance loss of a solar cell is estimated solely from the measured fill factor. In Fig. 9, the best efficiencies[11–15,135] of III–V compound MJ solar cells are also plotted. Two, three, four, five, and six-junction solar cells have potential efficiencies of 36.6%, 44.0%, 48.8%, 50.4%, and 51.4%, respectively, as shown in Fig. 9. Table I shows major losses, the origins of III–V compound MJ solar cells, and the key technologies for improving efficiency. As shown in Table I, further development of MJ solar cells is necessary in order to realize optimum efficiencies.

Other MJ solar cells composed of II–VI, chalcopyrite, kesterite compound, and perovskite solar cells are thought to have similar potential as III–V compound MJ solar cells. In order to realize high-efficiency MJ solar cells using these materials, reducing non-radiative recombination and resistance losses by learning from the progress achieved in III–V compound MJ solar cells is necessary.

TABLE I. Major losses, their origins of III–V compound MJ solar cells, and key technologies for improving efficiency. Reproduced with permission from M. Yamaguchi, "Fundamentals and R&D status of III-V compound solar cells and materials," Phys. Status Solidi C **12**, 489 (2015). Copyright 2015 Wiley.

Losses	Origins	Technologies for improving
Bulk recombination loss	Non-radiative recombination centers (impurities, dislocations, other defects)	High-quality epitaxial growth Reducing thermal stress Reduction in the density of defects
Surface recombination loss	Surface states	Surface passivation Heterointerface layer Double heterostructure (sandwitched with higher bandgap barrier layer)
Interface recombination loss	Interface states Lattice mismatching defects	Lattice matching Inverted epitaxial growth Back-surface field layer Double heterostructure
Voltage loss	Non-radiative recombination	Reduction in the density of defects
Resistance loss	Shunt resistance Series resistance Shunt resistance Loss of sub-cell interconnection	Thin absorber layers Reduction in contact resistance Reduction in leakage current, surface, interface passivation Reduction in sub-cell interconnection loss
Optical loss	Reflection loss Insufficient absorption	Anti-reflection coating, texture Back reflector, photon recycling
Insufficient energy photon loss	Spectral mismatching	Selection of sub-cell materials

2. Cost analysis of MJ solar cells

The allowable cost per unit area of solar cell modules largely depends on module efficiency.[137,138] For example, a 30%-efficient solar cell costing 3.5 times as much as a 15%-efficient solar cell of the same area will yield equivalent overall photovoltaic system costs[137] due to the balance of system costs. Therefore, high-efficiency solar cells will have a substantial economic advantage over low-efficiency solar cells, as the cost of fabricating the former is low enough. Additionally, efficiency improves the environmental impact of photovoltaic modules as less materials are needed to produce them. For space applications, high-efficiency solar cells have significant payload advantages. Although the III–V MJ solar cells have demonstrated an extremely high conversion efficiency with up to 39.2%,[15] further cost reduction is still necessary to access terrestrial photovoltaic markets.

Figure 10 shows a comparison of expected module costs as a function of module production volume for III–V tandem cells with/without high-speed deposition, III–V/Si tandem devices, and concentrators reported by the authors[138] and cost analytical results for rapid deposition (HVPE; Hydride Vapor Phase Epitaxy)[139] and Si tandem[17] reported by NREL. Therefore, ways for module cost reduction are reduction in film thickness, a high growth rate of the III–V layers, reuse of substrates, concentration of light, use of Si as substrate material and bottom cells, and an increase in module production volume, as shown in Fig. 10. The results suggest that there are ways to realize costs of less than \$1/W for III–V compound MJ solar cell modules by scaling up the production volume to 100 MW/year with a high-speed growth method or with Si-based tandem solar cells. Many of these technologies are current fields of research.

Cost analysis of perovskite and perovskite/Si tandem solar cell modules has been reported.[140,141] About \$0.5/W, comparable with crystalline Si and CdTe solar cell modules, was estimated as a manufacturing cost of perovskite and perovskite/Si tandem solar cell modules. One highly uncertain aspect of the module cost for

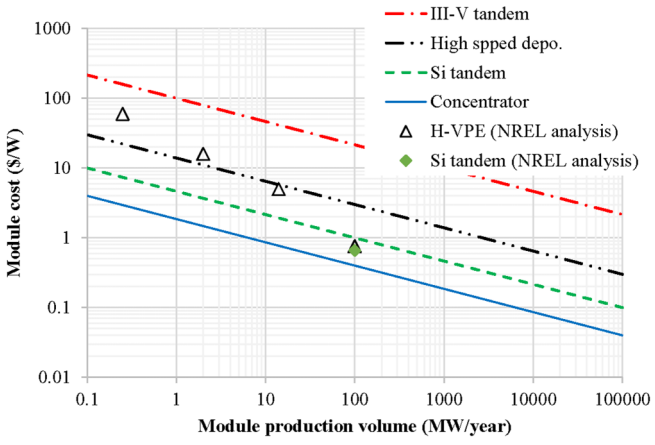

FIG. 10. A comparison of module cost as a function of module production volume for III–V tandem, high-speed deposition, Si tandem, and concentrator reported by the authors and cost analytical results for rapid deposition (HVPE; Hydride Vapor Phase Epitaxy) and Si tandem reported by NREL. Reproduced with permission from J. Crystal Growth **136**, 29 (1994). Copyright 1994, Elsevier.

tandem solar cell modules is the level of encapsulation that will be required to maintain tolerable module performance with a module efficiency of 24% over the working lifetime, 30 years.[140] For a silicon tandem, the underlying silicon cell degradation is generally low (less than 0.5%/year) with standard encapsulation methods, but it is not known what level of encapsulation will be required to deliver long-term efficient operation from perovskite on silicon tandem solar cells. What has been established is that the degradation rate of the top cell should be below 0.9%/year for a silicon tandem to remain financially viable.[142]

B. Perspective for MJ solar cells

Of all the so-called third generation solar cell strategies,[8] only MJ designs have been successful to surpass the detailed-balance limit of single-junction solar cells. Table II shows potential efficiencies of 3rd generation solar cells.[8,143–145] Demonstrated efficiencies of III–V MJ solar cells at one-sun are nearing levels of 40% and those under concentration are approaching levels of 50%. Most of the underlying physics of these cells have been understood, but sophisticated engineering and high-quality materials are an essential prerequisite for achieving higher levels of efficiency. While low-cost solar cell materials are desirable for tandem solar cells, only high-voltage junctions, as quantified by the ERE,[26,146] with well-chosen bandgaps matched to the application spectra will be helpful for surpassing the efficiency of single-junction silicon. Quantification of spectral efficiency[147] is a convenient metric to judge how to choose tandem partners, and more comprehensive multi-junction models are also available.[148] The challenge for low-cost tandem materials is to bring the best together in a way that preserves the high-quality junctions. This has already been achieved in high-efficiency III–V multi-junction devices, but here, lower processing costs are needed without compromising on the required quality for flat-plate areas. Alternatively, renewed development of robust and economical terrestrial concentrator systems could result in high demand for the most efficient multi-junction solar cells possible. The continued development of multi-junction solar strategies through multiple pathways and a sufficiently large market is likely to bring the technology closer to the economics of single-junction silicon and to provide clean, economical, and efficient energy, especially for area constrained applications.

TABLE II. Potential one-sun AM1.5 g efficiencies of 3rd generation solar cells.

Concept	Potential efficiency (%)	Achieved efficiency
Hot carrier solar cells	68	11.1% @50 000-suns (Ref. 142)
Tandem (multi-junction) solar cells (n→∞)	68	39.2% (n = 6) (Ref. 15) 47.1% @143-suns (n = 6) (Ref. 15)
Thermophotovoltaic solar cells	54	29.1% at an emitter temperature of 1207 °C (Ref. 143)
Tandem solar cells (n = 3)	49	37.9% (Ref. 12) 44.4% @300-suns (Ref. 12)
Impurity band solar cells (quantum dot solar cells)	48	18.7% (Ref. 144)
Tandem solar cells (n = 2)	43	32.8% (Ref. 1) 35.5% @38-suns (Ref. 1)
Single-junction solar cells	31	29.1% (Ref. 1) 30.5% @258-suns (Ref. 1)

C. Perspective for Si-based tandem solar cells

It can be expected that silicon-based tandem solar cells will receive further growing attention by the photovoltaic industry as efficiencies for single-junction solar cells reach a plateau and many of the opportunities for cost reduction have already been implemented. Innovation will most likely come from more efficient devices, and it has already been shown that Si-based tandem solar cells can achieve nearly 36% conversion efficiency in a two- or four-terminal configuration. This proves that Si-based tandem cells can get close to the best triple-junction solar cells ever reported in the literature and radiative efficiency limits are even as high as 45.2%, 49.6%, and 52.2% for two-junction, three-junction, and four-junction cells,[80] leaving sufficient room for further development. Using combinations of silicon and III–V materials allows the PV industry to keep many established processes that have already been scaled to large volumes. But at the same time new processes must be implemented and scientists will continue to have different opinions on which technologies are favorable for silicon-based tandem solar cells. The market will accept all those solutions that provide sufficiently high efficiencies combined with economically attractive production processes. We believe that III–V/silicon tandem solar cells will have a significant efficiency advantage compared with conventional silicon single-junction devices, and although they will be more expensive when they enter the market, their costs will reduce over a period of time. The exact efficiency number for market entry may be debatable, but probably it is on the order of 30% (AM1.5g) or more. The reduction in costs will depend on the market size, as indicated in Fig. 10, but for this to materialize, entry markets must be found. An example is electric cars where the high performance of the solar cells directly translates into longer driving distances before re-charging of the battery. Such conveniences often convince companies and customers to pay a premium price.

The simplest solution to realize a III–V/silicon tandem solar cell is a two-terminal device where the GaAsP top cell is grown directly onto a silicon bottom junction. The silicon junction may be formed by diffusion or implantation of P, GaP serves as a front surface field, and the rear may be formed by a combination of a SiO_x passivation with a nanostructured grating for light diffraction. Aluminum can be sputtered and point contacts formed by laser firing. Such a device would fulfill the requirements of manufacturability and low cost, but their performance is today still falling behind a good silicon single- junction solar cell. This may certainly change in the next coming years as defects in the III–V epitaxial layers are better controlled and issues with the GaP passivation to silicon solved. But it may also be necessary to develop more complex device architectures implementing III–V layer transfer

from a GaAs substrate, tunnel oxide passivation for silicon, four-terminal architectures, or additional junctions. Some of these approaches have already helped achieve up to 36% efficiency, but they suffer from disadvantages in terms of manufacturability and cost. Finding a path toward realizing a III–V/silicon tandem product will remain the subject of continued discussion in the coming years. But we can be confident that once performance and cost are shown to be economically attractive, nothing will stop the large-scale growth of this technology. The reliability of this technology should be comparable to silicon solar cells and presently, there seems to be no restriction to scale manufacturing to the GW level. Also, presently, there seems to be no restriction to scale manufacturing at the GW level.

V. CONCLUSION

In order to realize a society fully based on renewable energy, solar cells with the highest efficiency are attractive because they reduce the required system area and the need for using materials. As single-junction solar cells are limited to 30%–32% conversion efficiency under one-sun, MJ or tandem solar cells are expected to contribute to higher performances. The concept of MJ solar cells was first and most successfully implemented using III–V compound semiconductors and such products have already become the standard technology in space. There is a need to further improve their conversion efficiency of III–V MJ solar cells and reduce their cost to achieve widespread terrestrial deployment. At the same time, perovskite materials have emerged as an alternative solution to form MJ devices, but reliability, module integration, and large volume manufacturing are still subjects of current research and development.

In this paper, we provide perspectives for MJ solar cells from the viewpoints of efficiency and low-cost potential based on scientific and technological arguments and possible market applications. Two, three, four, five, and six-junction solar cells have potential efficiencies of 36.6%, 44.0%, 48.8%, 50.4%, and 51.4% under one-sun, respectively. For realizing higher efficiency MJ solar cells, we highlighted the importance of improving the external radiative efficiency of solar cell materials, or in other words, improving material quality and decreasing defect density in the bulk and at interfaces. Further decreasing resistance losses and applying light management for better absorption or photon recycling are important objectives to accomplish. There is a wide range of technological options under development that will lead to further efficiency improvement; most of these options revolve around target III–V MJ solar cells, III–V/Si, II–VI/Si, and perovskite/Si tandem solar cells. The potential for <1 $/W MJ solar cell modules exists for III–V based devices if new technologies such as high-speed deposition, Si-based tandem solar cells, or the use of concentration are employed with high efficiency and manufacturability. Once the technology is exposed to some terrestrial markets, cost reduction will happen, driven by an increase in production volumes. The history of the silicon photovoltaic industry bears testimony to this. So, the main question now is how to make the technology enter the terrestrial markets with volumes on the order of several hundred MW/year. Besides the III–Vs, other materials may have advantages in terms of production cost and they may enter the field of multi-junction technology quickly once the materials show high external radiative efficiency and reliability. II–VI/Si, chalcopyrite/Si , and especially perovskite/Si tandem solar cells, are being developed rapidly and are expected to play an important role as high-efficiency and low-cost solar cells in the future. As ideal bandgap combinations with the highest efficiency, MJ solar cells are often found in lattice-mismatched systems, and effecting efficiency improvements by making reductions in bulk recombination based on a further understanding of non-radiative recombination is necessary. Reduction in surface and interface recombination, efficient optical coupling and low loss electrical interconnection of sub-cells, and effective photon recycling of bottom solar cells are also key elements for high-efficiency MJ solar cells. At this point, nobody can predict which concept will be the most successful, but we firmly believe that at least one multi-junction solar cell technology with efficiency beyond the limits of silicon will emerge as a major player in the photovoltaic market. The only questions at this point of time are which materials will take the lead in this direction and when will this happen.

ACKNOWLEDGMENTS

M.Y., F.D., J.G. and N.J. wish to express thanks to the NEDO, EC, DOE and ARENA, respectively for their support.

DATA AVAILABILITY

The data that support the findings of this study are available from the corresponding author upon reasonable request.

REFERENCES

[1]M. A. Green, E. D. Dunlop, J. Hohl-Ebinger, M. Yoshita, N. Kopiakis, and X. Hao, "Solar cell efficiency tables (version 57)," Prog. Photovoltaics **29**, 3 (2021).
[2]M. Yamaguchi, "Fundamentals and R&D status of III-V compound solar cells and materials," Phys. Status Solidi C **12**, 489 (2015).
[3]W. Shockley and H. J. Queisser, "Detailed balance limit of efficiency of p-n junction solar cells," J. Appl. Phys. **32**, 510 (1961).
[4]M. Yamaguchi, T. Takamoto, K. Araki, and N. Ekins-Daukes, "Multi-junction III–V solar cells: Current status and future potential," Sol. Energy **79**, 78 (2005).
[5]M. Yamaguchi, "Super-high-efficiency III-V tandem and multi-junction cells," in *Clean Electricity from Photovoltaics*, 2nd ed., edited by M. D. Archer and M. A. Green (Imperial College Press, 2015), p. 307.
[6]L. C. Hirst and N. J. Ekins-Daukes, "Fundamental losses in solar cells," Prog. Photovoltaics **19**, 286 (2011).
[7]M. Yamaguchi, "High-efficiency GaAs-based solar cells," in *Gallium Arsenide*, edited by T. Tabbakh (IntechOpen, 2020).
[8]M. A. Green, "Third generation photovoltaics: Ultra-high conversion efficiency at low cost," Prog. Photovoltaics **9**, 123 (2001).
[9]E. D. Jackson, "Areas for improving of the semiconductor solar energy converter," in *Transzation Conference on the Use of Solar Energy* (University of Arizona Press, Tucson, 1958), Vol. 5, p. 122.
[10]M. Wolf, "Limitations and possibilities for improvement of photovoltaic solar energy converters," Proc. Inst. Radio Eng. **48**, 1246 (1960).
[11]N. Jain, K. L. Schulte, J. F. Geisz *et al.*, "High-efficiency inverted metamorphic 1.7/1.1 eV GaInAsP/GaInAs dual-junction solar cells," Appl Phys. Lett. **112**, 053905 (2018).
[12]K. Sasaki, T. Agui, K. Nakaido, N. Takahashi, R. Onitsuka, and T. Takamoto, "Development of InGaP/GaAs/InGaAs inverted triple junction concentrator solar cells," AIP Conf. Proc. **l556**, 22 (2013).

[13]F. Dimroth, T. N. D. Tibbits, M. Niemeyer, F. Predan, P. Beutel, C. Karcher, E. Oliva, G. Siefer, D. Lackner, P. Fus-Kailuweit, A. W. Bett, R. Krause, C. Drazek, E. Guiot, J. Wasselin, A. Tauzin, and T. Signamarcheix, "Four-junction waferbonded concentrator solar cells," IEEE J. Photovoltaics **6**, 343 (2016).
[14]P. T. Chiu, D. C. Law, R. L. Woo, S. B. Singer, D. Bhusari, W. D. Hong, A. Zakaria, J. Boisvert, S. Mesropian, R. R. King, and N. H. Karam, "35.8% space and 38.8% terrestrial 5J direct bonded cells," in *Proceedings of the 40th IEEE Photovoltaic Specialist Conference* (IEEE, New York, 2014), p. 11.
[15]J. F. Geisz, R. M. France, K. L. Schulte, M. A. Steiner, A. G. Norman, H. L. Guthrey, M. R. Young, T. Song, and T. Moriarty, "Six-junction III-V solar cells with 47.1% conversion efficiency under 143 suns concentration," Nat. Energy **5**, 326 (2020).
[16]M. Yamaguchi, K.-H. Lee, K. Araki, and N. Kojima, "A review of recent progress in heterogeneous silicon tandem solar cells," J. Phys. D: Appl. Phys. **51**, 133002 (2018).
[17]S. Essig, C. Allebe, T. Remo, J. F. Geisz, M. A. Steiner, K. Horowitz, L. Barraud, J. S. Ward, M. Schnabel, A. Descoeudres, D. L. Young, M. Woodhouse, M. Despeisse, C. Ballif, and A. Tamboil, "Raising the one-sun conversion efficiency of III–V/Si solar cells to 32.8% for two junctions and 35.9% for three junctions," Nat. Energy **2**, 17144 (2017).
[18]D. Lackner, O. Höhn, R. Müller, P. Beutel, P. Schygulla, H. Hauser, F. Predan, G. Siefer, M. Schachtner, J. Schön, J. Benick, M. Hermle, and F. Dimroth, "Two-terminal direct wafer-bonded GaInP/AlGaAs//Si triple-junction solar cell with AM1.5g efficiency of 34.1%," Sol. RRL **4**, 2000210 (2020).
[19]M. Carmody, S. Mallick, J. Margetis, R. Kodama, T. Biegala, D. Xu, P. Bechmann, J. W. Garland, and S. Sivananthan, "Single-crystal II-VI on Si single-junction and tandem solar cells," Appl. Phys. Lett. **96**, 153502 (2010).
[20]K. Kim, J. Gwak, S. K. Ahn, Y.-J. Eo, J. H. Park, J.-S. Cho, M. G. Kang, H.-E. Song, and J. H. Yun, "Simulations of chalcopyrite/c-Si tandem cells using SCAPS-1D," Sol. Energy **145**, 52 (2017).
[21]M. Valentini, C. Malerba, L. Serenelli, M. Izzi, E. Salza, M. Tucci, and A. Mittiga, "Fabrication of monolithic CZTS/Si tandem cells by development of the intermediate connection," Sol. Energy **190**, 414 (2019).
[22]S. Albrecht, A. Al-Asgouri, E. Kohnen, M. Jost, L. Kegelmann, A. Morales, T. Bertram, L. Korte, B. Stannowski, C. Kaufmann, and R. Schlatmann, paper presented at the 36th European Photovoltaic Solar Energy Conference, Marseille, France, 2019.
[23]R. Lin, K. Xiao, Z. Y. Qin, Q. Han, C. Zhang, M. Wei, M. L. Saidaminov, Y. Gao, J. Xu, M. Xiao, A. Li, J. Zhu, E. H. Sargent, and H. Tan, "Monolithic all-perovskite tandem solar cells with 24.8% efficiency exploiting comproportionation to suppress Sn (II) oxidation in precursor ink," Nat. Energy **4**, 864 (2019).
[24]K. Makita, H. Mizuno, T. Tayagaki, T. Aihara, R. Oshima, Y. Shoji, H. Sai, H. Takato, R. Müller, P. Beutel, D. Lackner, J. Benick, M. Hermle, F. Dimroth, and T. Sugaya, "III-V//Si multijunction solar cells with 30% efficiency using smart stack technology with Pd nanoparticle array," Prog. Photovolt: Res. Appl. vol. 42, no. 8, 2019.
[25]S. Buecheler, F. Fu, T. Feurer, S. Pisoni, E. Avancini, R. Carron, S. Nishiwaki, and A. N. Tiwari, paper presented at the 7th International Workshop on CIGS Solar Cell Technology, Munich, Germany, 23 June 2016.
[26]U. Rau, "Reciprocity relation between photovoltaic quantum efficiency and electroluminescent emission of solar cells," Phys. Rev. B **76**, 085303 (2007).
[27]M. A. Green, "Time-asymmetric photovoltaics," Nano Lett. **12**, 5985 (2012).
[28]H. Mashaal and J. Gordon, "Basic limit for the efficiency of coherence-limited solar power conversion," Opt. Lett. **39**, 5130 (2014).
[29]S. R. Kurtz, P. Faine, and J. M. Olson, "Modeling of 2-junction, series-connected tandem solar-cells using top-cell thickness as an adjustable-parameter," J. Appl. Phys. **68**, 1890 (1990).
[30]N. L. A. Chan, T. B. Young, H. E. Brindley, N. J. Ekins-Daukes, K. Araki, Y. Kemmoku, and M. Yamaguchi, "Validation of energy prediction method for a concentrator photovoltaic module in Toyohashi Japan," Prog. Photovoltaics **21**, 1598 (2012).
[31]M. A. Steiner, J. F. Geisz, I. Garcia *et al.*, "Optical enhancement of the open-circuit voltage in high quality GaAs solar cells," J. Appl. Phys. **113**, 123109 (2013).
[32]F. Staub, I. Anusca, D. C. Lupascu, U. Rau, and T. Kirchartz, "Effect of reabsorption and photon recycling on photoluminescence spectra and transients in lead-halide perovskite crystals," J. Phys. Mater. **3**, 025003 (2020).
[33]C. Baur, M. Hermle, F. Dimroth, and A. W. Bett, "Effects of optical coupling in III-V multilayer systems," Appl. Phys. Lett. **90**, 192109 (2007).
[34]M. A. Steiner, J. F. Geisz, T. E. Moriarty, R. M. France, W. E. McMahon, J. M. Olson, S. R. Kurtz, and D. J. Friedman, "Measuring IV curves and subcell photocurrents in the presence of luminescent coupling," IEEE J. Photovoltaics **3**, 879 (2013).
[35]N. L. A. Chan, T. Thomas, M. Fuhrer, and N. J. Ekins-Daukes, "Practical limits of multi-junction solar cell performance enhancement from radiative coupling considering realistic spectral conditions," IEEE J. Photovoltaics **4**, 1306 (2014).
[36]D. J. Friedman, J. F. Geisz, and M. A. Steiner, "Effect of luminescent coupling on the optimal design of multi-junction solar cells," IEEE J. Photovoltaics **4**, 986 (2014).
[37]A. Pusch, P. Pearce, and N. J. Ekins-Daukes, "Analytical expressions for the efficiency limits of radiatively coupled tandem solar cells," IEEE J. Photovoltaics **9**, 679 (2019).
[38]W. Walukiewicz, K. M. Yu, J. Wu *et al.*, U.S. patent 7,217,882 B2 (15 May 2007).
[39]M. Niemeyer, J. Ohlmann, A. W. Walker, P. Kleinschmidt, R. Lang, T. Hannappel, F. Dimroth, and D. Lackne, "Minority carrier diffusion length, lifetime and mobility in p-type GaAs and GaInAs," J. Appl. Phys. **122**, 115702 (2017).
[40]J. M. Gee, "A comparison of different module configurations for multi-band-gap solar cell," Sol. Cells **24**, 147–155 (1988).
[41]M. J. Ludowise, U.S. patent 4,575,576 (11 March 1986).
[42]S. M. Bedair, "Algaas tunnel diode," J. Appl. Phys. **50**, 7267 (1979).
[43]M. Yamaguchi, C. Amano, H. Sugiura, and A. Yamamoto, "High efficiency AlGaAs-GaAs tandem solar cells with tunnel junction," in *Proceedings of the 19th IEEE Photovoltaic Specialists Conference* (IEEE, New York, 1987), p. 1484.
[44]C. H. Henry, "Limiting efficiencies of ideal single and multiple energy gap terrestrial solar cells," J. Appl. Phys. **51**, 4494–4500 (1980).
[45]A. Marti and G. L. Araujo, "Limiting efficiencies for photovoltaic energy conversion in multigap systems," Sol. Energy Mater. Sol. Cells **43**, 203–222 (1996).
[46]W. E. McMahon, D. J. Friedman, and J. F. Geisz, "Multi-junction solar cell design revisited: Disruption of current-matching by atmospheric absorption bands," Prog. Photovoltaics Res. Appl. **25**, 850–860 (2017).
[47]A. Al-Ashouri, E. Köhnen, B. Li, A. Magomedov, H. Hempel, P. Caprioglio, J. A. Márquez, A. B. Morales Vilches, E. Kasparavicius, J. A. Smith, N. Phung, D. Menzel, M. Grischek, L. Kegelmann, D. Skroblin, C. Gollwitzer, T. Malinauskas, M. Jošt, G. Matič, B. Rech, R. Schlatmann, M. Topič, L. Korte, A. Abate, B. Stannowski, D. Neher, M. Stolterfoht, T. Unold, V. Getautis, and S. Albrecht, "Monolithic perovskite/silicon tandem solar cell with >29% efficiency by enhanced hole extraction," Science **370**, 1300 (2020).
[48]R. L. Moon, L. W. James, H. A. Vander Plas *et al.*, "Multigap solar cell requirements and the performance of AlGaAs and Si cells in concentrated sunlight," in *Proceedings of the 13th IEEE PVSC* (IEEE, 1978), pp. 859–867.
[49]S. M. Bedair, J. A. Hutchby, J. Chiang *et al.*, "AlGaAs/GaAs high efficiency cascade solar cells," in *Proceedings of the 15th IEEE Photovoltaic Specialists Conference* (IEEE, 1981), pp. 21–26.
[50]B.-C. Chung, G. F. Virshup, and J. C. Schultz, "27.6% (1-sun, air mass 1.5 G) monolithic two-junction AlGaAs/GaAs solar cell and 25% (1-sun, air mass 0) three junction AlGaAs/GaAs/InGaAs cascade solar cell," in *Proceedings of the 21st IEEE PVSC* (IEEE, 1990), pp. 179–183.
[51]K. Ando, C. Amano, H. Sugiura, M. Yamaguchi, and A. Saletes, "Nonradiative e-h recombination characteristics of mid-gap electron trap in AlxGa1-xAs (x = 0.4) grown by MBD," Jpn. J. Appl. Phys. **26**, L266–L269 (1987).

[52]G. B. Stringfellow, "The importance of lattice mismatch in the growth of $Ga_xIn_{1-x}P$ epitaxial crystals," J. Appl. Phys. **43**, 3455–3460 (1972).
[53]J. M. Olson, T. Gessert, and M. M. Al-Jassim, "GaInP2/GaAs: A current- and lattice-matched tandem cell with a high theoretical efficiency," in *Proceedings of the 18th IEEE Photovoltaic Specialists Conference* (IEEE, 1985), pp. 552–555.
[54]L. C. Su, S. T. Pu, G. B. Stringfellow *et al.*, "Control of ordering in GaInP and effect on bandgap energy," J. Electron. Mater. **23**, 125–133 (1994).
[55]D. J. Friedman, J. F. Geisz, S. R. Kurtz *et al.*, "1-eV solar cells with GaInNAs active layer," J. Cryst. Growth **195**, 409–415 (1998).
[56]D. B. Jackrel, S. R. Bank, H. B. Yuen *et al.*, "Dilute nitride GaInNAs and GaInNAsSb solar cells by molecular beam epitaxy," J. Appl. Phys. **101**, 114916 (2007).
[57]V. Sabnis, H. Yuen, and M. Wiemer, "High-efficiency multi-junction solar cells employing dilute nitrides," AIP Conf. Proc. **1477**, 14 (2012).
[58]C. L. Andre, J. J. Boeckl, D. M. Wilt *et al.*, "Impact of dislocations on minority carrier electron and hole lifetimes in GaAs grown on metamorphic SiGe substrates," Appl. Phys. Lett. **84**, 3447–3449 (2004).
[59]M. W. Wanlass, J. F. Geisz, S. Kurtz *et al.*, "Lattice-mismatched approaches for high performance III-V photovoltaic energy converters," in *Proceedings of the Proceedings of the 31st IEEE Photovoltaic Specialists Conference*, Orlando, FL (IEEE, 2005), pp. 530–535.
[60]J. F. Geisz, D. J. Friedman, J. S. Ward *et al.*, "40.8% efficient inverted triple-junction solar cell with two independently metamorphic junctions," Appl. Phys. Lett. **93**, 123505 (2008).
[61]J. F. Geisz, S. R. Kurtz, M. W. Wanlass *et al.*, "High-efficiency GaInP/GaAs/InGaAs triple-junction solar cells grown inverted with a metamorphic bottom junction," Appl. Phys. Lett. **91**, 023502 (2007).
[62]R. M. France, J. F. Geisz, I. García *et al.*, "Quadruple junction inverted metamorphic concentrator devices," IEEE J. Photovoltaics **5**, 432–437 (2015).
[63]R. M. France, "Design flexibility of ultra-high efficiency 4-junction inverted metamorphic solar cells," in *Proceedings of the 42nd IEEE PVSC*, New Orleans (IEEE, 2015).
[64]R. Tatavarti, G. Hillier, A. Dzankovic *et al.*, "Lightweight, low cost GaAs solar cells on 4″ epitaxial liftoff (ELO) wafers," in *Proceedings of the 33rd Photovoltaic Specialists Conference*, San Diego, CA (IEEE, 2008), pp. 1–4.
[65]T. Takamoto, H. Washio, and H. Juso, "Application of InGaP/GaAs/InGaAs triple junction solar cells to space use and concentrator photovoltaic," in *Proceedings of the 40th IEEE PVSC*, Denver, CO (IEEE, 2014), pp. 0001–0005.
[66]O. D. Miller, E. Yablonovitch, and S. R. Kurtz, "Strong internal and external luminescence as solar cells approach the Shockley-Queisser limit," IEEE J. Photovoltaics **2**, 303–311 (2012).
[67]S Wojtczuk, P. T. Chiu, X. Zhang *et al.*, "InGaP/GaAs/InGaAs 41% concentrator cells using bi-facial epigrowth," in *Proceedings of the 35th IEEE Photovoltaic Conference*, Honolulu, HI (IEEE, 2010), pp. 1259–1264.
[68]M. A. Steiner, R. M. France, J. Buencuerpo, J. F. Geisz, M. P. Nielsen, A. Pusch, W. J. Olavarria, M. Young, and N. J. Ekins-Daukes, "High efficiency inverted GaAs and GaInP/GaAs solar cells with strain-balanced GaInAs/GaAsP quantum wells," Adv. Energy Mater. **11**, 2002874 (2021).
[69]W. Guter, J. Schone, S. P. Philipps *et al.*, "Current-matched triple-junction solar cell reaching 41.1% conversion efficiency under concentrated sunlight," Appl. Phys. Lett. **94**, 223504 (2009).
[70]R. R. King, D. C. Law, K. M. Edmondson *et al.*, "40% efficient metamorphic GaInP/GaInAs/Ge multi-junction solar cells," Appl. Phys. Lett. **90**, 183516 (2007).
[71]R. H. van Leest, D. Fuhrmann, A. Frey, M. Meusel, G. Siefer, and S. K. Reichmuth, "Recent progress of multi-junction solar cell development for CPV applications at AZUR SPACE," AIP Conf. Proc. **2149**, 020007 (2019).
[72]A. Mukhtarova, S. Valdueza-Felip, L. Redaelli, C. Durand, C. Bougerol, E. Monroy, and J. Eymery, "Dependence of the photovoltaic performance of pseudomorphic InGaN/GaN multiple-quantum-well solar cells on the active region thickness," Appl. Phys. Lett. **108**, 161907 (2016).
[73]Z. Q. Li, M. Lestradet, Y. G. Xiao, and S. Li, "Effects of polarization change on the photovoltaic properties of InGaN solar cells," Phys. Status Solidi A **208**, 928 (2011).
[74]P. D. C. King, T. D. Veal, H. Lu, P. H. Jefferson, S. A. Hatfield, W. J. Schaff, and C. F. McConville, "Surface electronic properties of n- and p-type InGaN alloys (journal article) surface electronic properties of n- and p-type InGaN alloys," Phys. Status Solidi B **245**, 881 (2008).
[75]R. Singh, D. Doppalapudi, T. D. Moustakas, and L. T. Romano, "Phase separation in InGaN thick films and formation of InGaN/GaN double heterostructures in the entire alloy composition," Appl. Phys. Lett. **70**, 1089 (1997).
[76]A. Bhuiyan, K. Sugita, A. Hashimoto, and A. Yamamoto, "InGaN solar cells: Present state of the art and important challenges," IEEE J. Photovoltaics **2**, 276 (2012).
[77]K. Yoshikawa, H. Kawasaki, W. Yoshida, T. Irie, K. Konishi, K. Nakano, T. Uto, D. Adachi, M. Kanematsu, H. Uzu, and K. Yamamoto, "Silicon heterojunction solar cell with interdigitated back contacts for a photoconversion efficiency over 26%," Nat. Energy **2**, 17032 (2017).
[78]A. Richter, M. Hermle, and S. W. Glunz, "Reassessment of the limiting efficiency for crystalline silicon solar cells," IEEE J. Photovoltaics **3**, 1184–1191 (2013).
[79]B. A. Veith-Wolf, S. Schäfer, R. Brendel, and J. Schmidt, "Reassessment of intrinsic lifetime limit in n-type crystalline silicon and implication on maximum intrinsic lifetime limit in n-type crystalline silicon" Sol. Energy Mater. Sol. Cells **186**, 194–199 (2018).
[80]P. Schygulla and F. Dimroth, "Unpublished calculations of the radiative efficiency limit for III-V/silicon tandem solar cells performed with the program ETA-OPT: G. Létay and A. W. Bett, 'EtaOpt—A program for calculating limiting efficiency and optimum bandgap structure for multi-bandgap solar cells and TPV cells'," in Proceedings of the 17th European Photovoltaic Solar Energy Conference and Exhibition, WIP, Munich, Germany (2001), pp. 178–181
[81]N. Tucher, O. Höhn, J. C. Goldschmidt, and B. Bläsi, "Optical modeling of structured silicon-based tandem solar cells and module stacks," Opt. Express **26**, A761 (2018).
[82]J. Eisenlohr, B. G. Lee, J. Benick, F. Feldmann, M. Drießen, N. Milenkovic, B. Bläsi, J. C. Goldschmidt, and M. Hermle, "Rear side sphere gratings for improved light trapping in crystalline silicon single junction and silicon-based tandem solar cells," Sol. Energy Mater. Sol. Cells **142**, 60–65 (2015).
[83]Z. Liu, Z. Ren, H. Liu, J. P. Mailoa, N. Sahraei, S. Siah, F. Lin, T. Buonassisi, and I. M. Peters, "Light management in mechanically-stacked GaAs/Si tandem solar cells: Optical design of the Si bottom cell," in *Proceedings of the 42nd IEEE Photovoltaic Specialist Conference* (IEEE, New York, 2001), p. 1.
[84]H. Sai, Y. Kanamori, K. Arafune, Y. Ohshita, and M. Yamaguchi, "Light trapping effect of submicron surface textures in crystalline Si solar cells," Prog. Photovoltaics **15**, 415 (2007).
[85]J. M. Gee, "Optically enhanced absorption in thin silicon layers using photonic crystals," in *Proceedings of the 29th IEEE Photovoltaic Specialist Conference* (IEEE, New York, 2001), p. 150.
[86]R. Dewan and D. Knipp, "Light-trapping in thin-film silicon solar cells with integrated diffraction grating," J. Appl. Phys. **106**, 074901 (2009).
[87]T. J. Grassman, D. J. Chmielewski, S. D. Carnevale, J. A. Carlin, and S. A. Ringel, "$GaAs_{0.75}P_{0.25}$/Si dual-junction solar cells grown by MBE and MOCVD," IEEE J. Photovoltaics **6**, 326–331 (2016).
[88]S. Fan, Z. J. Yu, R. D. Hool, P. Dhingra, W. Weigand, M. Kim, E. D. Ratta, B. D. Li, Y. Sun, Z. C. Holman, and M. L. Lee, "Epitaxial GaAsP/Si solar cells with high quantum efficiency," in *2020 47th IEEE Photovoltaic Specialists Conference (PVSC)*, Calgary, OR (IEEE, 2020), pp. 2370–2373.
[89]See https://www.ise.fraunhofer.de/en/press- media/press-releases/2021/tandem-photovoltaics-enables-new-heights-in-solar-cell- efficiencies-35point9-percent-for-iii-v-silicon-solar-cell.html for "Press Release Fraunhofer ISE—23.4.2021."
[90]R. Müller, P. Schygulla, D. Lackner, O. Höhn, H. Hauser, A. Richter, A. Fell, B. Bläsi, F. Predan, J. Benick, M. Hermle, F. Dimroth, and S. W. Glunz, "Silicon-based monolithic triple-junction solar cells with conversion efficiency >34%" in 37th European Photovoltaic Solar Energy Conference and Exhibition, WIP, virtual event (2020) to be published.
[91]P. Demeester, I. Pollentier, P. De Dobbelaere, C. Brys, and P. V. Daele, "Epitaxial lift-off and its applications," Semicond. Sci. Technol. **8**, 1124 (1993).

[92]J. T. Boyer, A. N. Blumer, Z. H. Blumer, D. L. Lepkowski, and T. J. Grassman, "Reduced dislocation introduction in III–V/Si heterostructures with glide-enhancing compressively strained superlattices," Cryst. Growth Des. **20**(10), 6939–6946 (2020).
[93]D. L. Lepkowski, T. Kasher, T. J. Grassman and S. A. Ringel, "Designing an Epitaxially-Integrated DBR for Dislocation Mitigation in Monolithic GaAsP/Si Tandem Solar Cells," in IEEE Journal of Photovoltaics, vol. 11, no. 2, pp. 400–407.
[94]Y. Vaynzof, "The future of perovskite photovoltaics—Thermal evaporation or solution processing," Adv. Energy Mater. **10**, 2003073 (2020).
[95]M. Jošt, L. Kegelmann, L. Korte, and S. Albrecht, "Monolithic perovskite tandem solar cells: A review of the present status and advanced characterization methods toward 30% efficiency," Adv. Energy Mater. **10**, 1904102 (2020).
[96]J. Tong, Q. Jiang, F. Zhang, S. B. Kang, D. H. Kim, and K. Zhu, "Wide-bandgap metal halide perovskites for tandem solar cells," ACS Energy Lett. **6**, 232 (2020).
[97]N. Liu, L. Wang, F. Xu, J. Wu, T. Song, and Q. Chen, "Recent progress in developing monolithic perovskite/Si tandem solar cells," Front. Chem. **8**, 603375 (2020).
[98]C. Messmer, B. S. Goraya, S. Nold, P. S. C. Schulze, V. Sittinger, J. Schön, J. C. Goldschmidt, M. Bivour, S. W. Glunz, and M. Hermle, "The race for the best silicon bottom cell: Efficiency and cost evaluation of perovskite–silicon tandem solar cells," Prog. Photovoltaics Res. Appl. 1–16 (2020).
[99]F. Sahli, J. Werner, B. A. Kamino, M. Bräuninger, R. Monnard, B. Paviet-Salomon, L. Barraud, L. Ding, J. J. Diaz Leon, D. Sacchetto, G. Cattaneo, M. Despeisse, M. Boccard, S. Nicolay, Q. Jeangros, B. Niesen, and C. Ballif, "Fully textured monolithic perovskite/silicon tandem solar cells with 25.2% power conversion efficiency," Nat. Mater. **17**, 820 (2018).
[100]Y. Hou, E. Aydin, M. De Bastiani, C. Xiao, F. H. Isikgor, D. J. Xue, B. Chen, H. Chen, B. Bahrami, A. H. Chowdhury, A. Johnston, S. W. Baek, Z. Huang, M. Wei, Y. Dong, J. Troughton, R. Jalmood, A. J. Mirabelli, T. G. Allen, E. Van Kerschaver, M. I. Saidaminov, D. Baran, Q. Qiao, K. Zhu, S. De Wolf, and E. H. Sargent, "Efficient tandem solar cells with solution-processed perovskite on textured crystalline silicon," Science **367**, 1135 (2020).
[101]R. Carron, S. Nishiwaki, T. Feurer, R. Hertwig, E. Avancini, J. Löckinger, S. Yang, S. Buecheler, and A. N. Tiwari, "Advanced alkali treatments for high-efficiency Cu(In,Ga)Se_2 solar cells on flexible substrates," Adv. Energy Mater. **9**, 1900408 (2019).
[102]T. Todorov, T. Gershon, O. Gunawan, Y. S. Lee, C. Sturdevant, L.-Y. Chang, and S. Guha, "Monolithic perovskite-CIGS tandem solar cells via *in situ* band Gap engineering," Adv. Energy Mater. **5**, 1500799 (2015).
[103]Q. Han, Y. T. Hsieh, L. Meng, J. L. Wu, P. Sun, E. P. Yao, S. Y. Chang, S. H. Bae, T. Kato, V. Bermudez, and Y. Yang, "High-performance perovskite/Cu(In,Ga)Se_2 monolithic tandem solar cells," Science **361**, 904 (2018).
[104]A. Al-Ashouri, A. Magomedov, M. Roß, M. Jošt, M. Talaikis, G. Chistiakova, T. Bertram, J. A. Márquez, E. Köhnen, E. Kasparavičius, S. Levcenco, L. Gil-Escrig, C. J. Hages, R. Schlatmann, B. Rech, T. Malinauskas, T. Unold, C. A. Kaufmann, L. Korte, G. Niaura, V. Getautis, and S. Albrecht, "Conformal monolayer contacts with lossless interfaces for perovskite single junction and monolithic tandem solar cells," Energy Environ. Sci. **12**, 3356 (2019).
[105]E. Bellini, see https://www.pv-magazine.com/2020/04/16/hzb-scientists-announce-24-16- efficiency-for-tandem-cigs-solar-cell/ for "HZB scientists announce 24.16% efficiency for tandem CIGS solar cell" (2020).
[106]J. Im, C. C. Stoumpos, H. Jin, A. J. Freeman, and M. G. Kanatzidis, "Antagonism between spin-orbit coupling and steric effects causes anomalous band gap evolution in the perovskite photovoltaic materials $CH_3NH_3Sn_{1-x}Pb_xI_3$," J. Phys. Chem. Lett. **6**, 3503 (2015).
[107]R. Lin, K. Xiao, Z. Qin, Q. Han, C. Zhang, M. Wei, M. I. Saidaminov, Y. Gao, J. Xu, M. Xiao, A. Li, J. Zhu, E. H. Sargent, and H. Tan, "Monolithic all-perovskite tandem solar cells with 24.8% efficiency exploiting comproportionation to suppress Sn(II) oxidation in precursor ink," Nat. Energy **4**, 864 (2019).
[108]G. Li, W.-H. Chang, and Y. Yang, "Low-bandgap conjugated polymers enabling solution-processable tandem solar cells," Nat. Rev. Mater. **2**, 170483 (2017).
[109]L. Meng, Y. Zhang, X. Wan, C. Li, X. Zhang, Y. Wang, X. Ke, Z. Xiao, L. Ding, and R. Xia, "Organic and solution-processed tandem solar cells with 17.3% efficiency," Science **361**, 1094 (2018).
[110]M. Bär, W. Bohne, J. Röhrich, E. Strub, S. Lindner, M. C. Lux-Steiner, C.-H. Fischer, T. P. Niesen, and F. Karg, "Determination of the band gap depth profile of the penternary $Cu(In_{(1-x)}Ga_X)(S_YSe_{(1-Y)})_2$ chalcopyrite from its composition gradient," J. Appl. Phys. **96**, 3857 (2004).
[111]X. Wu, J. Zhou, A. Duda, J. C. Keane, T. A. Gessert, Y. Yan, and R. Noufi, "13·9%-efficient CdTe polycrystalline thin-film solar cells with an infrared transmission of ~50," Prog. Photovoltaics Res. Appl. **14**, 471 (2006).
[112]M. Schmid, R. Caballero, R. Klenk, J. Krč, T. Rissom, M. Topi, and M. C. Lux-Steiner, "Experimental verification of optically optimized $CuGaSe_2$ top cell for improving chalcopyrite tandems," EPJ Photovoltaics **1**, 10601 (2010).
[113]K. Makita, H. Komaki, H. Mizuno, H. Sai, T. Sugaya, R. Oshima, H. Shibata, K. Matsubara, and S. Niki. "A 24.2%-efficiency III-V/CuInGaSe mechanical stacking multi-junction solar cells using semiconductor bonding method," in 29th European Photovoltaic Solar Energy Conference and Exhibition, WIP (2014)," 1427–1429.
[114]G. M. Hanket, J. H. Boyle, and W. N. Shafarman, "Characterization and device performance of (AgCu)(InGa)Se_2 absorber layers," in *2009 34th IEEE Photovoltaic Specialists Conference (PVSC)* (IEEE, 2009), p. 001240.
[115]K. Kim, S. K. Ahn, J. H. Choi, J. Yoo, Y.-J. Eo, J.-S. Cho, A. Cho, J. Gwak, S. Song, D.-H. Cho, Y.-D. Chung, and J. H. Yun, "Highly efficient Ag-alloyed Cu(In,Ga)Se_2 solar cells with wide bandgaps and their application to chalcopyrite-based tandem solar cells," Nano Energy **48**, 345 (2018).
[116]K. Kim, J. S. Yoo, S. K. Ahn, Y.-J. Eo, J.-S. Cho, J. Gwak, and J. H. Yun, "Performance prediction of chalcopyrite-based dual-junction tandem solar cells," Sol. Energy **155**, 167 (2017).
[117]Y. Zhou, L. Wang, S. Chen, S. Qin, X. Liu, J. Chen, D.-J. Xue, M. Luo, Y. Cao, Y. Cheng, E. H. Sargent, and J. Tang, "Thin-film Sb_2Se_3 photovoltaics with oriented one-dimensional ribbons and benign grain boundaries," Nat. Photonics **9**, 409 (2015).
[118]R. Tang, X. Wang, W. Lian, J. Huang, Q. Wei, M. Huang, Y. Yin, C. Jiang, S. Yang, G. Xing, S. Chen, C. Zhu, X. Hao, M. A. Green, and T. Chen, "Hydrothermal deposition of antimony selenosulfide thin films enables solar cells with 10% efficiency," Nat. Energy **5**, 587 (2020).
[119]J. Zhang, W. Lian, Y. Yin, X. Wang, R. Tang, C. Qian, X. Hao, C. Zhu, and T. Chen, "All antimony chalcogenide tandem solar cell," Solar RRL **4**, 2000048 (2020).
[120]A. B. Nikolskaia, M. F. Vildanova, S. S. Kozlov, and O. I. Shevaleevskiy, "Two-terminal tandem solar cells DSC/c-Si: Optimization of TiO_2-based photoelectrode parameters," Semiconductors **52**, 88 (2018).
[121]A. Pusch and N. J. Ekins-Daukes, "Voltage matching, ětendue and ratchet steps in advanced-concept solar cells," Phys. Rev. Appl. **12**, 044055 (2019).
[122]T. Trupke and P. Wurfel, "Improved spectral robustness of triple tandem solar cells by combined series/parallel interconnection," J. Appl. Phys. **96**, 2347 (2004).
[123]L. M. Pazos-Outón, J. M. Lee, M. H. Futscher, A. Kirch, M. Tabachnyk, R. H. Friend, and B. Ehrler, "A silicon-singlet fission tandem solar cell exceeding 100% external quantum efficiency with high spectral stability," ACS Energy Lett. **2**, 476 (2017).
[124]M. Einzinger, T. Wu, J. F. Kompalla, H. L. Smith, C. F. Perkinson, L. Nienhaus, S. Wieghold, D. N. Congreve, A. Kahn, M. G. Bawendi, and M. A. Baldo, "Sensitization of silicon by singlet exciton fission in tetracene," Nature **571**, 90 (2019).
[125]R. W. MacQueen, M. Liebhaber, J. Niederhausen, M. Mews, C. Gersmann, S. Jäckle, K. Jäger, M. J. Y. Tayebjee, T. W. Schmidt, B. Rech, and K. Lips, "Crystalline silicon solar cells with tetracene interlayers: The path to silicon-singlet fission heterojunction devices," Mater. Horiz. **5**, 1065 (2018).
[126]J. J. Loferski, "Tandem photovoltaic solar cells and increased energy conversion efficiency," in *Conference Record of the 12th IEEE Photovoltaic Specialists Conference*, Baton Rouge (IEEE, Piscataway, 1976), p. 957.

[127]M. F. Lamorte and D. H. Abbott, "Computer modeling of a two-junction monolithic cascade solar cell," IEEE Trans. Electron Devices **27**, 831 (1980).
[128]K. W. Mitchell, "High efficiency concentrator cells," in *Conference Record of the 15th IEEE Photovoltaic Specialists Conference*, Kissimmee (IEEE, Piscataway, 1981), p. 142.
[129]J. C. C. Fan, B. Y. Tsaur, and B. J. Palm, "Optical design of high-efficiency tandem cells," in *Proceedings of the 16th IEEE Photovoltaic Specialists Conference* (IEEE, New York, 1982), p. 692.
[130]M. E. Nell and A. M. Barnett, "The spectral p-n junction model for tandem solar-cell design," IEEE Trans. Electron Devices **34**, 257 (1987).
[131]C. Amano, H. Sugiura, M. Yamaguchi, and K. Hane, "Fabrication and numerical analysis of AlGaAs/GaAs tandem solar cells with tunnel interconnections," IEEE Trans. Electron Devices **36**, 1026 (1989).
[132]G. Letay and A. W. Bett, "Theoretical investigation III–V multi-junction solar cells," in *Proceedings of the 17th European Photovoltaic Solar Energy Conference* (WIP, Munich, 2001), p. 178.
[133]S. P. Philipps and A. W. Bett, "III-V multi-junction solar cells," in *Advanced Conception Photovoltaics*, edited by A. J. Nozik, G. Conibeer, and M. Beard (Royal Society of Chemistry, 2014), p. 87.
[134]A. Vossier, E. Al Alam, A. Dollet, and M. Amara, "Assessing the efficiency of advanced multi-junction solar cells in real working conditions: A theoretical analysis," IEEE J. Photovoltaics **5**, 1 (2015).
[135]B. M. Kayes, H. Nie, R. Twist, S. G. Spruytte, F. Reinhardt, I. C. Kizilyalli, and G. S. Higashi, "27.6% conversion efficiency, a new record for single-junction solar cells under 1 sun illumination," in *Proceedings of the 37th IEEE Photovoltaic Conference* (IEEE, New York, 2011), p. 4.
[136]M. Yamaguchi, K. H. Lee, K. Araki, N. Kojima, H. Yamada, and Y. Katsumata, "Analysis for efficiency potential of high-efficiency and next generation solar cells," Prog. Photovoltaics **26**, 543 (2018).
[137]D. L. Bowler and M. Wolf, "Interactions of efficiency and material requirements for terrestrial silicon solar cells," in *IEEE Transactions on Components, Hybrids, and Manufacturing Technology, CHMT-3* (IEEE, 1980), p. 464.
[138]M. Yamaguchi, T. Warabisako, and H. Sugiura, "CBE as a breakthrough technology for PV solar energy applications," J. Cryst. Growth **136**, 29 (1994).
[139]K. A. W. Horowitz, T. Remo, B. Smith, and A. Ptak, "Techno-economic analysis and cost reduction roadmap for III-V solar cell," NREL Technical Report 2018. NREL/TP- 6A20-72103, November 2018, see https://www.nrel.gov/docs/fy19osti/72103.pdf.
[140]N. L. Chang, A. W. Yi Ho-Baillie, P. A. Basore, T. L. Young, R. Evans, and R. J. Egan, "A manufacturing cost estimation method with uncertainty analysis and its application to perovskite on glass photovoltaic modules," Prog. Photovoltaics **25**, 390 (2017).
[141]Z. Li, Y. Zhao, X. Wang, Y. Sun, Z. Zhao, Y. Li, H. Zhou, and Q. Chen, "Cost analysis of perovskite tandem photovoltaics," Joule **2**, 1559 (2018).
[142]J. Qian, M. Ernst, N. Wu, and A. Blakers, "Impact of perovskite solar cell degradation on the lifetime energy yield and economic viability of perovskite/silicon tandem modules," Sustain. Energy Fuels **3**, 1439 (2019).
[143]D.-T. Nguyen, L. Lombez, F. Gibelli, S. Boyer-Richard, A. Le Corre, O. Durand, and J.-F. Guillemoles, "Quantitative experimental assessment of hot carrier-enhanced solar cells at room temperature," Nat. Energy **3**, 236 (2018).
[144]Z. Omair, G. Scranton, L. M. Pazos-Outón, T. P. Xiao, M. A. Steiner, V. Ganapati, P. F. Peterson, J. Holzrichter, H. Atwater, and E. Yablonovitch, "Ultraefficient thermophotovoltaic power conversion by band-edge spectral filtering," Proc. Natl. Acad. Sci. U.S.A. **116**, 15356 (2019).
[145]K. Tanabe, D. Guimard, D. Bordel, and Y. Arakawa, "High-efficiency InAs/GaAs quantum dot solar cells by metalorganic chemical vapor deposition," Appl. Phys. Lett. **100**, 193905 (2012).
[146]M. A. Green, "Radiative efficiency of state-of-the-art photovoltaic cells," Prog. Photovoltaics **20**, 472 (2012).
[147]Z. Yu, M. Leilaeioun, and Z. Holman, "Selecting tandem partners for silicon solar cells," Nat. Energy **1**, 16137 (2016).
[148]J. F. Geisz, M. A. Steiner, I. Garcia *et al.*, "Generalized optoelectronic model of series-connected multi-junction solar cells," IEEE J. Photovoltaics **5**, 1827 (2015).